High-Level ab Initio Calculations on the Gas-Phase Reactions between $C^+(^2P)$ and Formic Acid

Ana I. González, Alberto Luna, and Manuel Yáñez*

Departamento de Química, C-9, Universidad Autónoma de Madrid, Cantoblanco, 28049 Madrid, Spain

Received: February 15, 1999

The $[H_2, C_2, O_2]^+$ potential energy surface was explored through the use of G2 high-level ab initio calculations. The global minimum can be viewed as the result of inserting the C^+ monocation into the C═O bond of formic acid. However, the products of the C^+ + HCOOH reactions do not arise from the unimolecular decomposition of this species, but from the structures that correspond to the attachment of C^+ either to the carbonyl oxygen atom or to the OH group of the neutral. Both attachment processes are almost equally exothermic and yield HCO^+, $HCO^•$, and $COH^•$ as dominant products. This is in agreement with the fact that HCO^+ is the sole product molecular ion detected in this reaction. The unimolecular decomposition of the global minimum would yield, as the dominant product, the $HCOH^+$ cation, which is not experimentally observed. This is consistent with our results, which show that this process cannot compete with the previous ones. The two functional groups present in formic acid perturb each other to a significant extent, and C^+ + formic acid reactions present some interesting peculiarities with respect to C^+ + formaldehyde and C^+ + methanol reactions. Significant differences are also observed with respect to the analogous Si^+ reactions.

Introduction

In the last few years our group has been interested in the study of gas-phase reactions involving open-shell monocations.[1] These processes are quite often a challenge for the theory, since the treatment of open-shell systems may present complications that are not usually found when dealing with closed-shell species.[1,2] The reactions involving $C^+(^2P)$ ions are particularly interesting because many of them are involved in the formation of new species in the interstellar space, where $Si^+(^2P)$ is also a relatively abundant species.[3,4] This moved us to undertake a systematic study of different reactions involving these two monocations and different neutral systems. In previous work we have found that there are significant differences in the reactivity of C^+ and Si^+. In fact, we have shown that while the most stable molecular ion when Si^+ interacts with formaldehyde[1i] corresponds to the adduct of the monocation to the carbonyl oxygen, in the formaldehyde−C^+ interactions[1j] the global minimum of the potential energy surface (PES) corresponds to the insertion of the monocation into the C═O bond of the neutral. On the other hand, the global minimum of the methanol−Si^+ PES[1k] corresponds to the insertion of the monocation into the C−OH bond of the neutral while that of the methanol−C^+ PES[1i] corresponds to a $H_2\dot{C}$−$CHOH^+$ distonic ion. Also, interestingly, in silanol−C^+ interactions the insertion of C^+ into the OH linkage is more favorable than the insertion into the Si−OH bond.[1k]

These differences in gas-phase reactivities are also reflected in significant dissimilarities in the corresponding charge distributions. Actually, we have found that while the adduct of Si^+ to the C═O bond of formaldehyde ($H_2\dot{C}$═OSi^+) is a distonic ion,[1i] the adduct of C^+ (H_2C═OC^+) is not,[1j] and vice versa, while the insertion of Si^+ into the C═O bond of formaldehyde yields a nondistonic (H_2C−Si−O^+) ion, the insertion of C^+ yields a distonic one ($H_2\dot{C}$−C−O^+).

There are also significant differences in the binding energies depending on the functional group to which the monocation is attached. Actually, the attachment of Si^+ to the hydroxyl group of methanol[1k] was predicted to be 8.0 kcal/mol less exothermic than its attachment to the carbonyl group of formaldehyde; but when both functional groups coincide in the same neutral, as in formic acid,[1m] the gap between the estimated binding energies becomes more than twice as large. One obvious question will be if something similar is expected for formic acid−C^+ reactions. To answer this question as well as to offer plausible mechanisms for the formation of the experimentally observed products,[5] we have explored, in this paper, the PES associated with such a reaction through the use of high-level ab initio techniques.

Computational Details

The $[H_2, C_2, O_2]^+$ doublet PES has been explored through the use of the G2 theory.[6] The G2 theory is a composite procedure based on the 6-311G(d,p) basis set and several basis extensions, where electron correlation effects are treated at the MP4 and QCISD(T) levels of theory. The final energies are effectively at the QCISD(T)/6-311+G(3df,2p) level, assuming that basis set effects on the correlation energies are additive. A small empirical correction (HLC) to accommodate remaining deficiencies is finally added as well as the corresponding zero point energy (ZPE) correction, estimated at the HF/6-31G* level. The reader is addressed to ref 6 for a complete description of this method. Also, recently, an assessment of the G2 theory for the computation of enthalpies of formation has been published.[7] Although in the standard G2 procedure the harmonic vibrational frequencies are evaluated at the HF/6-31G* level, in our case they have been obtained at the MP2(full)/6-31G* level and the corresponding ZPE corrections were scaled by the empirical factor 0.9646.[8] All these calculations have been carried out using the Gaussian-94[9] series of programs.

The interaction of $C^+(^2P)$ with formic acid leads to a drastic reorganization of the charge distribution of the whole system, which has been analyzed in terms of the atoms in molecules

10.1021/jp990545j CCC: $18.00
Published on Web 05/22/1999

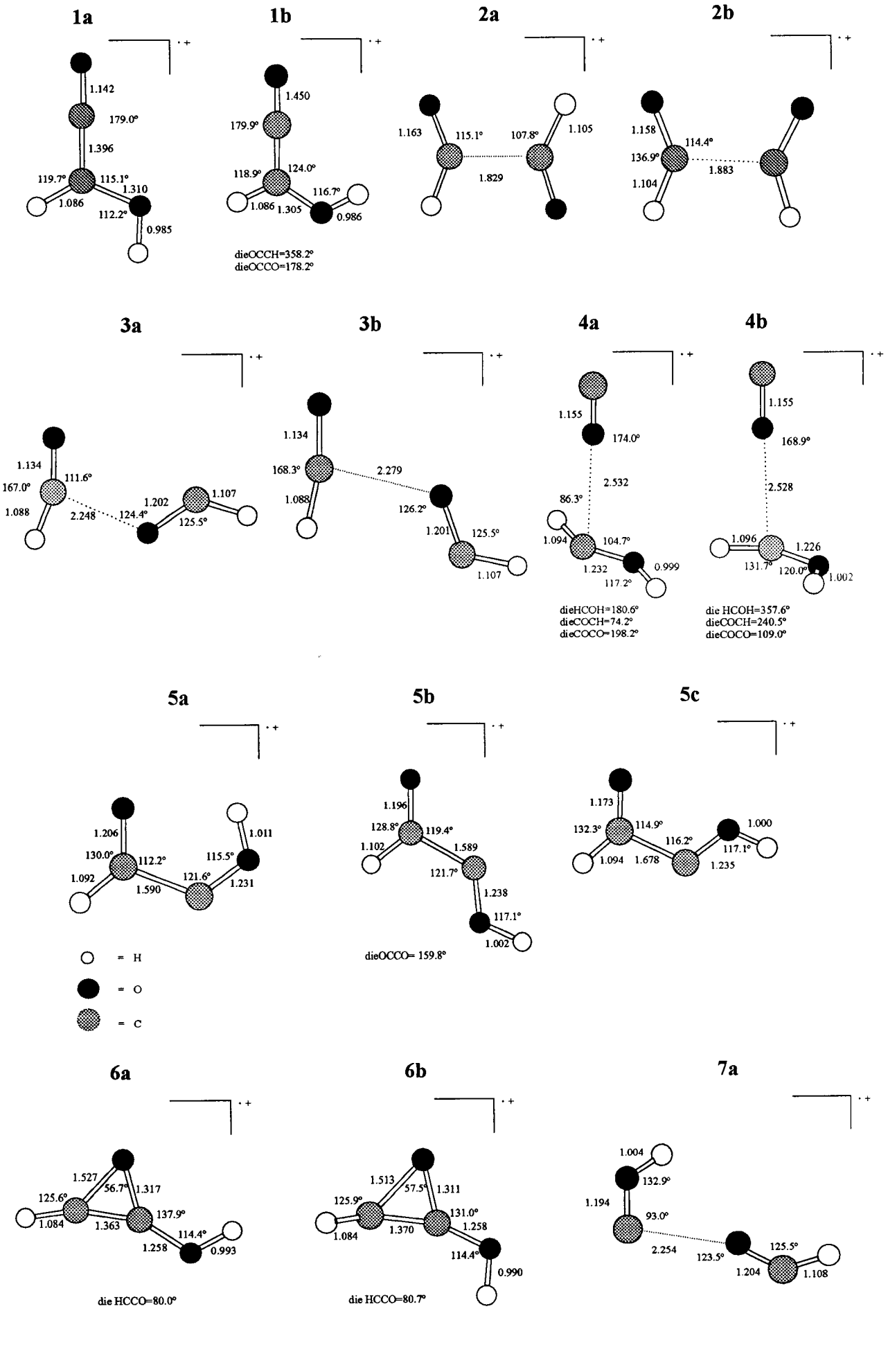
1a
1.142
179.0°
1.396
119.7°
115.1°
1.310
1.086
112.2°
0.985
1b
1.450
179.9°
118.9°
124.0°
116.7°
1.086
1.305
0.986
dieOCCH=358.2°
dieOCCO=178.2°
2a
1.163
115.1°
107.8°
1.105
1.829
2b
1.158
114.4°
136.9°
1.883
1.104
3a
1.134
111.6°
167.0°
1.088
2.248
124.4°
1.202
1.107
125.5°
3b
1.134
168.3°
2.279
1.088
126.2°
1.201
125.5°
1.107
4a
1.155
174.0°
2.532
86.3°
1.094
104.7°
1.232
0.999
117.2°
dieHCOH=180.6°
dieCOCH=74.2°
dieCOCO=198.2°
4b
1.155
168.9°
2.528
1.096
1.226
131.7°
120.0°
1.002
die HCOH=357.6°
dieCOCH=240.5°
dieCOCO=109.0°
5a
1.206
130.0°
112.2°
115.5°
1.011
1.092
121.6°
1.231
1.590
= H
= O
= C
5b
1.196
128.8°
119.4°
1.102
1.589
121.7°
1.238
117.1°
1.002
dieOCCO= 159.8°
5c
1.173
132.3°
114.9°
1.000
116.2°
117.1°
1.094
1.678
1.235
6a
1.527
56.7°
1.317
125.6°
1.084
1.363
137.9°
114.4°
1.258
0.993
die HCCO=80.0°
6b
1.513
57.5°
1.311
125.9°
131.0°
1.084
1.370
1.258
114.4°
0.990
die HCCO=80.7°
7a
1.004
132.9°
1.194
93.0°
2.254
123.5°
125.5°
1.204
1.108

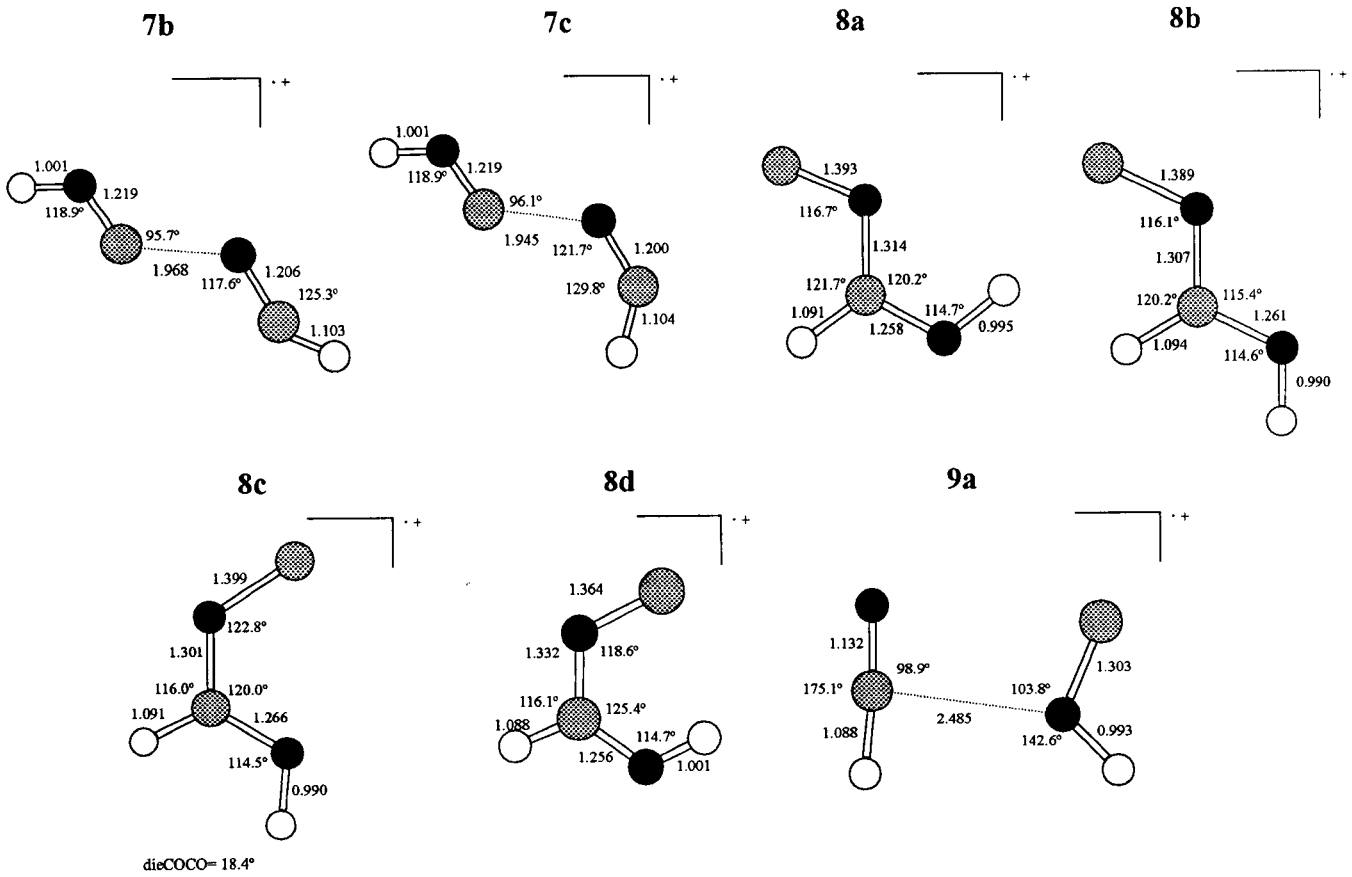

Figure 1. MP2(full)/6-31G* optimized geometries of the local minima of the $[H_2, C_2, O_2]^+$ PES. Bond lengths are in Ångstroms, and bond angles are in degrees.

(AIM) theory of Bader.[10] The AIM theory is based on a topological analysis of the electron charge density, $\rho(\mathbf{r})$, and its Laplacian, $\nabla^2\rho(\mathbf{r})$. More specifically, we have located the so-called bond critical points (bcps), i.e., points where $\rho(\mathbf{r})$ is minimum along the bond path and maximum in the other two directions. In general, the values of ρ and $\nabla^2\rho$ at these points provide useful information on the bonding characteristics of the system.

Since as mentioned above, electron correlation effects are crucial for the systems under study, this population analysis was performed at the MP2 level using the AIMPAC[11] series of programs.

Results and Discussion

The optimized geometries of the different minima located in the $[H_2, C_2, O_2]^+$ PES are given in Figure 1. The different minima were numbered in decreasing stability order. When a given isomer presents several conformations, these were distinguished by adding a, b, c, ... to the number that designates the isomer. Their total and relative energies are summarized in Table 1. This table also includes the $\langle S^2 \rangle$ expectation values for all the species investigated, just to show that in no case is the spin contamination of the unrestricted wave function significant.

Structures. It can be observed that the global minimum of the PES, **1a**, corresponds to the insertion of C^+ into the C═O bond of the neutral. The insertion of C^+ into the O—H bond of the formic acid results in a large activation of the C—OH linkage, which practically dissociates, yielding species **3a,b**, which can be viewed as tightly bound complexes between COH^+ and $COH^\bullet$. Species **2a,b**, which are slightly more stable than the previous ones, can be viewed as the result of a different rearrangement of the same two interacting moieties. It is also worth noting that species **2a,b** can alternatively be envisaged as the radical cation of dioxetane.

The insertion of the C^+ monocation into the C—OH bond yields species **5a**—**c**, while the insertion into the C—H bonds apparently leads to the formation of a COC three-membered ring (**6a**,**b**). However, an inspection of the topology of the electron charge density of these structures shows that there is no bond critical point between the CH group and the oxygen atom, and therefore the CH is only bonded to the other carbon atom. Consistently, these structures are distonic, the unpaired electron being associated with the CH carbon while the positive charge is located on the carbonyl carbon.

The attachment of C^+ to the carbonyl oxygen atom yields structures **8a**—**d**, which lie quite high in energy with respect to the insertion into the bond, which, as we mentioned above, is the global minimum of the PES. It is worth mentioning that structures **8** are clearly distonic since the unpaired electron is located at the terminal carbon atom, and the positive charge is mainly on the central carbon atom. The attachment of the C^+ monocation to the OH group yields, apparently, two kinds of structures, namely, **7a**—**c** and **9**. It is important to emphasize that this interaction implies a large activation of the C—OH bond, which practically dissociates. In principle, one may consider that the only difference between structures **7** and **9** is, as in the case of species **2** and **3**, the different rearrangements of the two interacting moieties. However, an inspection of their charge distributions reveals that they present completely different electronic configurations. In species **7** the unpaired electron appears associated with the HCO moiety, while the COH subunit

TABLE 1: Total G2 Energies (hartrees) and Relative Energies (kcal/mol) to the Global Minimum and the Value of $\langle S^2 \rangle$

species	E (G2)	ΔE	$\langle S^2 \rangle$
1a	−227.16652	0.0	0.790
1b	−227.16181	2.9	0.790
2a	−227.12954	23.2	0.840
2b	−227.12324	27.2	0.837
3a	−227.12382	26.8	0.763
3b	−227.12265	27.5	0.764
4a	−227.11056	35.1	0.759
4b	−227.10516	38.5	0.774
5a	−227.09589	44.3	0.765
5b	−227.09403	45.6	0.763
5c	−227.09231	46.6	0.765
6a	−227.09500	44.9	0.799
6b	−227.09465	45.1	0.803
7a	−227.05894	67.5	0.763
7b	−227.05588	69.4	0.764
7c	−227.05554	69.6	0.788
8a	−227.04762	74.6	0.761
8b	−227.04551	75.9	0.759
8c	−227.04517	76.1	0.764
8d	−227.04498	76.3	0.760
9	−227.04667	75.2	0.761
TS4a1a	−227.10564	38.2	0.759
TS8a9	−226.98193	115.8	0.767
TS1a5c	−227.04866	74.0	0.811
TS1b2a	−227.06007	66.8	0.832
TS1a1b	−227.15060	10.0	0.791
TS8d3a	−227.04167	78.3	0.761
TS8c9	−226.98751	112.3	0.772
TS8a7b	−226.98613	113.2	0.771
TS8a8d	−227.04240	77.9	0.763
HCOOH	−189.51647		
$HCO^{\bullet}$	−113.69870		
$COH^{\bullet}$	−113.63127		
HCO^{+}	−113.40344		
COH^{+}	−113.34174		
$HCOH^{\bullet +}$	−113.92649		
CO	−113.17779		

supports most of the positive charge of the system. In contrast, in species **9** the positive charge is located on the HCO moiety while the unpaired electron is associated with the COH subunit. On the other hand, if one takes into account that the energy of the $COH^{+} + HCO^{\bullet}$ noninteracting systems is 3.7 kcal/mol lower than that of $COH^{\bullet} + HCO^{+}$, it is reasonable to expect species **7** to be more stable than species **9**. All this would imply, in principle, that the attachment of C^{+} to the OH group can lead to two alternative heterolytic dissociations of the C−OH bond, depending in which moiety retains the bonding electron pair. When the bonding pair remains associated with the COH moiety, the products are $COH^{\bullet} + HCO^{+}$, and when they remain associated with the HCO subunit, the dissociation would yield $COH^{+} + HCO^{\bullet}$. However, when a C^{+} is approached to the OH group of the formic acid only structure **9** is formed. Furthermore, any attempt to optimize structure **9** by approaching COH^{+} and $HCO^{\bullet}$ failed. Hence, we must conclude that the attachment of C^{+} to the hydroxyl group of formic acid yields exclusively structure **9** and, as we shall discuss later, species **7** can be only generated from structure **8a** through an appropriate hydrogen transfer mechanism.

It is also interesting to note the existence of structures **4a,b**, which correspond to weakly bound complexes between carbon monoxide and the two isomers of the $HCOH^{+}$ molecular ion. These species are quite stable, reflecting the large stability of the CO molecule, and in principle could be the result of the dissociation of the C−OC bond of species **8**. However, as we shall discuss in forthcoming sections, it is not easy to establish reaction mechanisms connecting both structures.

Relative Stabilities. Formic Acid Reactions vs Formaldehyde and Methanol Reactions. As we have mentioned in the introduction, one of the goals of our study was to compare the C^{+} reactivity, with respect to a typical bidendate base as formic acid, with that exhibited by formaldehyde and methanol, where only one of the basic functional groups is present. For the sake of conciseness we are going to focus our attention on the reactions of attachment of C^{+} to the C═O and the OH groups and the insertion of C^{+} into the C═O and the C−OH bonds.

It is apparent from Figure 2 that the insertion of C^{+} into the C═O bond of formic acid is less exothermic than its insertion into the C═O bond of formaldehyde. This reflects the stabilization of the carbonyl group by OH substitution. As has been shown by Wiberg et al.,[12] electronegative substituents significantly stabilize the C═O function, and therefore one should expect the insertion into the C═O bond to be less favorable, from the energetic point of view, in formic acid than in formaldehyde. This is also consistent with the fact that the charge density at the C═O bond critical point is sizably larger in formic acid (0.408 au) than in formaldehyde (0.395 au).

Addition of C^{+} to the carbonyl group is also less exothermic in formic acid than in formaldehyde. This could be anticipated in terms of the smaller intrinsic basicity of this group when the hydrogen atom of formaldehyde is substituted by an electron-withdrawing OH group. Nevertheless, it is important to note that the basicity dampening of the carbonyl group dominates with respect to the reinforcement of the bond. Accordingly, while the energy gap between the insertion and the addition mechanisms is about 64 kcal/mol in formaldehyde, it becomes about 74 kcal/mol in formic acid.

Attachment of C^{+} to the OH group as well as its insertion into the C−OH linkage are also less exothermic than analogous processes in methanol The reasons are similar to those invoked above when discussing the addition and the insertion mechanisms to the C═O bond. The C−OH linkage becomes reinforced on going from methanol to formic acid, while the intrinsic basicity of the OH group decreases. However, in this case the first effect dominates and we found that the energy gap between insertion and addition mechanisms, which for methanol is about 70 kcal/mol, for formic acid is only about 29 kcal/mol.

It can also be observed that while the insertion of C^{+} into the C═O bond of formaldehyde is about 11 kcal/mol more exothermic than its insertion into the C−OH bond of methanol, in formic acid the energy gap between both processes (46.5 kcal/mol) increases dramatically.

The relative intrinsic basicities of the carbonyl and the hydroxyl groups are also affected when both functional groups coincide in the same system. As shown in Figure 2, attachment of C^{+} to the OH group of methanol is 18 kcal/mol less exothermic than addition to the C═O group of formaldehyde. However, in formic acid both attachment reactions are almost equally exothermic.

Comparison of C^{+} vs Si^{+}. We have considered it also of interest to compare the reactivity of C^{+} with that of Si^{+} when they interact with the same neutrals. The first important difference, as illustrated in Figure 2, is that in formic acid + Si^{+} reactions[1m] the addition of the monocation to the carbonyl oxygen is more exothermic than its insertion into the C═O bond, but more importantly, its insertion into the C−OH linkage is the most favorable process, leading to the global minimum of the PES. This is consistent, as shown in the same figure, with the fact that for Si^{+} reactions, the insertion of the monocation

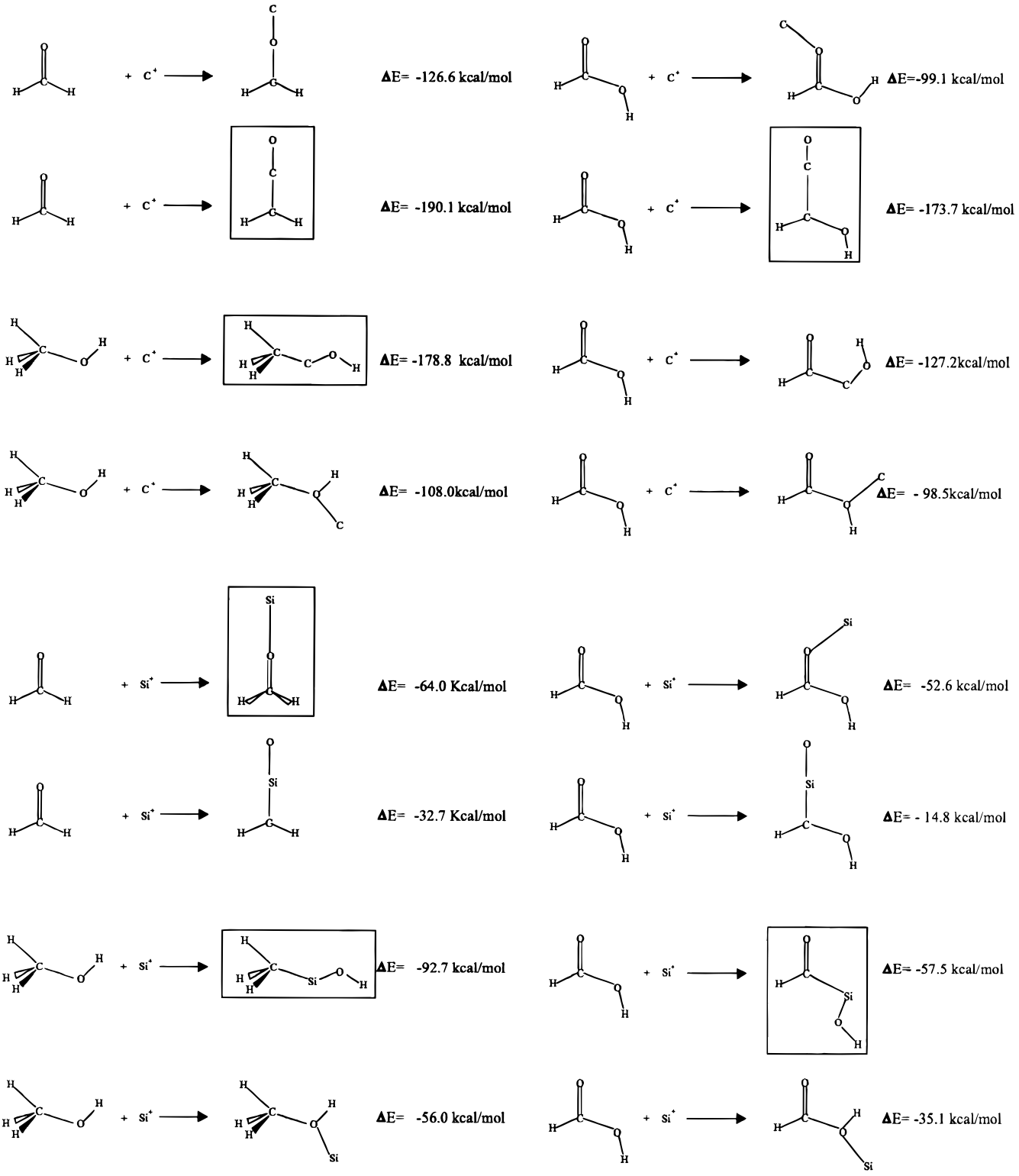

Figure 2. Energetics of the addition and insertion processes into the C═O and the C−OH bonds of formaldehyde, methanol, and formic acid in reactions with $C^+(^2P)$ and $Si^+(^2P)$. The global minimum of each reaction has been framed within a rectangle.

into the C−OH bond of methanol is more exothermic than its addition to the C═O group of formaldehyde.

Similarly to what was discussed above for C^+ reactions, the addition and insertion mechanisms in Si^+ + formic acid reactions are systematically less exothermic than the corresponding process associated with Si^+ + formaldehyde and Si^+ + methanol reactions. There are, however, some quantitative differences when the intrinsic basicities of carbonyl and hydroxyl groups are considered. For both C^+ and Si^+ the addition to the carbonyl group of formaldehyde is more exothermic than the addition to the hydroxyl group of methanol, but the energy gap is more than twice as large for C^+ (18.6 kcal/mol) as for Si^+ (8.0 kcal/mol). On the other hand, while this gap almost disappears in formic acid + C^+ reactions (0.6 kcal/mol), in formic acid + Si^+ reactions it increases significantly (17.5 kcal/mol).

Energy Profile of the Formic Acid + C^+ Reaction. The energy profile of the reaction between C^+ and formic acid is

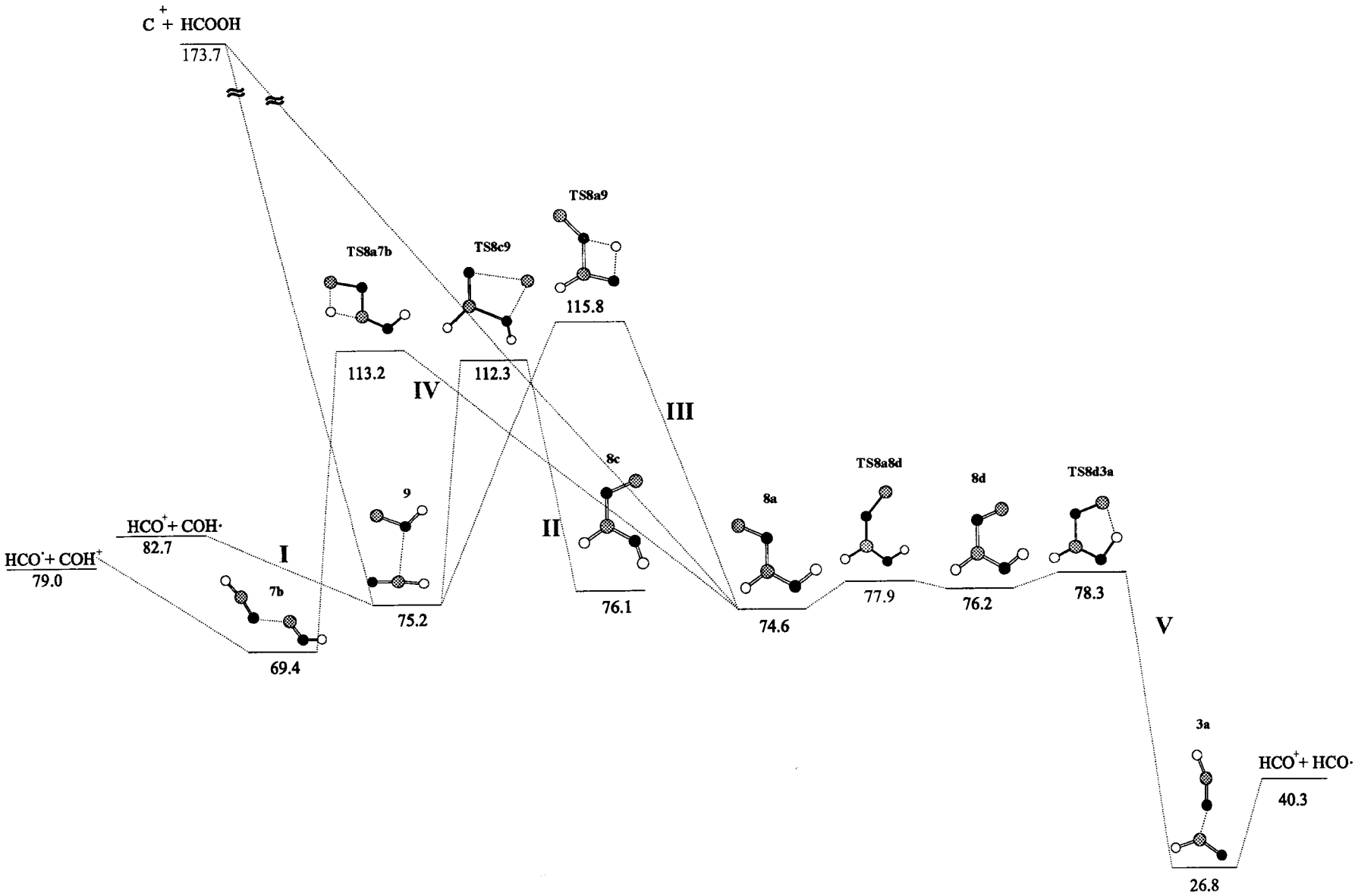

Figure 3. Energy profile of the $C^+(^2P)$ + formic acid reactions. Relative energies (in kcal/mol) referred to the global minimum.

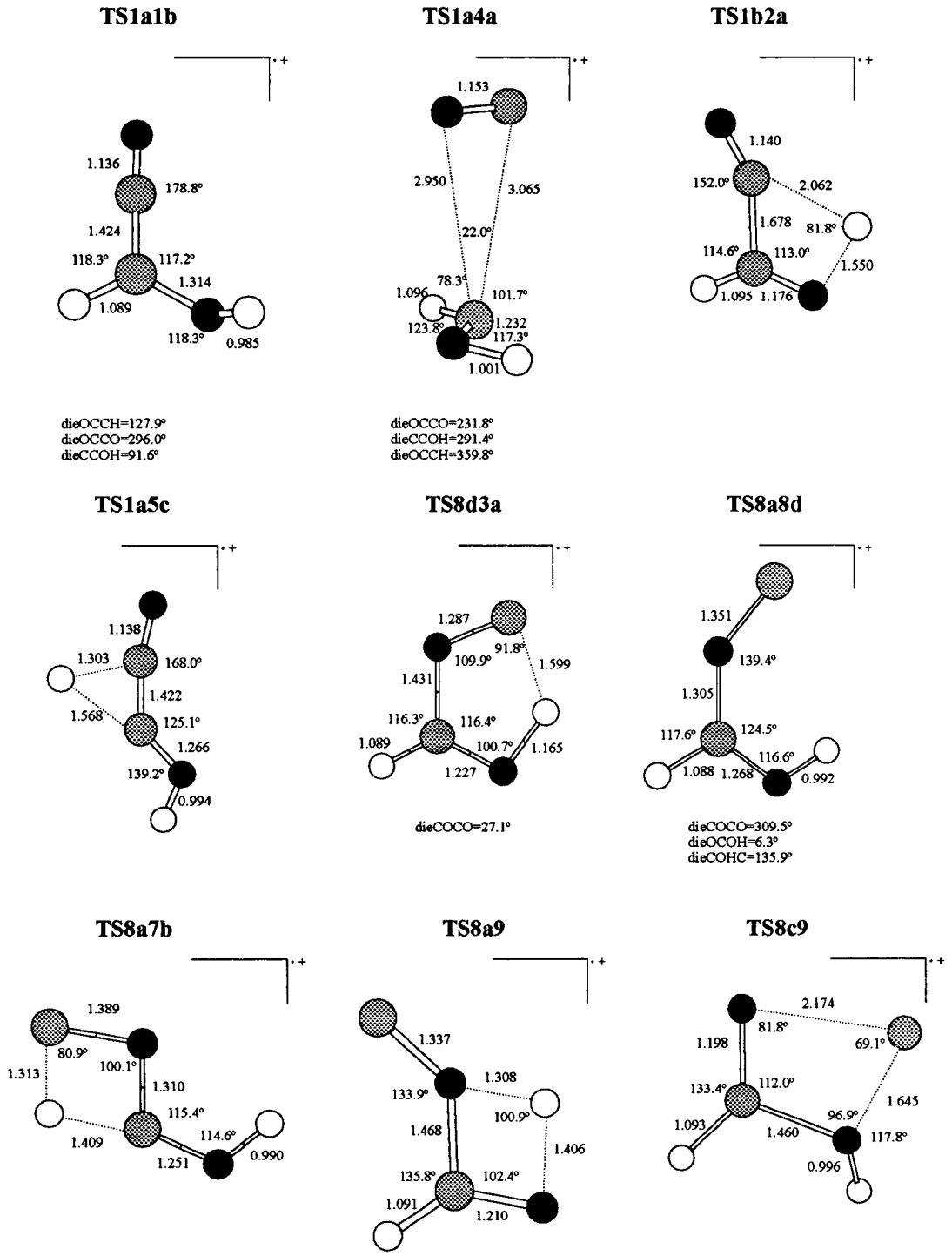

Figure 4. Optimized structures of the transition states located in the $[H_2, C_2, O_2]^+$ PES. Bond lengths are in in Ångstroms, and bond angles are in degrees.

presented in Figure 3. The structures of the different transition states that connect the different minima are given in Figure 4, and their energies, in Table 1.

It is reasonable to expect that the first step in the reaction between formic acid and C^+ in the gas phase would be the attachment of the monocation either to the carbonyl oxygen atom (to yield species **8a**−**d**) or to the hydroxyl oxygen (to yield species **9**). Since, as we have mentioned above, the first process is only slightly more favorable than the second one, the mechanisms with origins in species **8** and **9** are likely to be equally significant.

As we have discussed in previous sections, the attachment of C^+ to the OH group of formic acid leads to a C−OH bond fission, so that species **9** is an ion−dipole complex between HCO^+ and COH that lies 7.5 kcal/mol below the noninteracting products (mechanism I in Figure 3). On the other hand, species **9** can be alternatively formed from species **8c** by a carbon transfer process through the transition state **TS8c9** (mechanism II). A 1,3 hydrogen process through the **TS8a9** transition state would also connect species **8a** with structure **9** (mechanism III). All these mechanisms that involve as the final step the direct dissociation of structure **9** would yield $HCO^+ + COH^\bullet$ as products of the reaction.

A fourth alternative mechanism (IV in Figure 3) is associated with the 1,3H transfer that connects structures **8a** and **7b** through the **TS8a7b** transient species. As we have mentioned above,

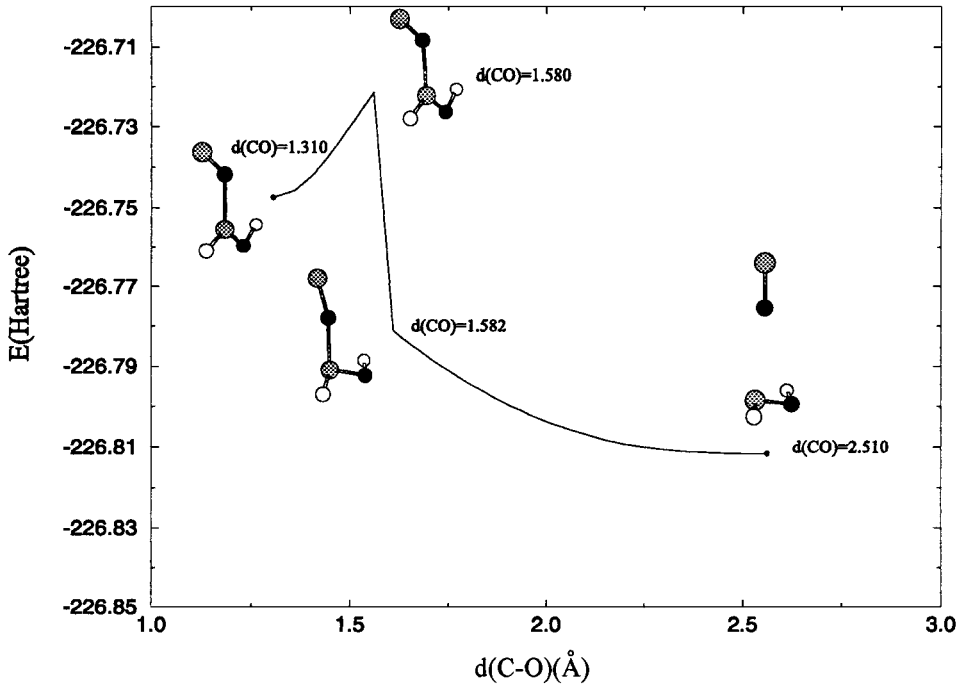

Figure 5. Potential energy curve associated with the lengthening of the C−OC bond of species **8a**. For each value of the reaction coordinate the remaining geometrical parameters were fully optimized at the MP2(full)/6-31G* level.

species **7b**, which is a $COH^+\cdots HCO^\bullet$ ion−dipole complex, will eventually dissociate into the two interacting subunits.

As illustrated in Figure 3, once the **8a** adduct is formed, its evolution through an internal rotation of the OC group to yield the **8d** conformer requires a low-energy barrier (mechanism V). A subsequent 1,4H transfer through the **TS8d3a** transition state would yield structure **3a**, which lies much lower in energy and which would eventually dissociate into $HCO^+ + HCO^\bullet$, which are the experimentally[5] observed products for this reaction.

It is evident from the values of the barriers shown in Figure 3, that mechanisms II, III, and IV cannot compete with mechanisms I and V. It is also apparent that mechanism V is the most favorable one, since it originates from the most stable adduct and implies the lowest activation barriers. This is in nice agreement with the experimental results that found $HCO^+ + HCO^\bullet$ as the only products of the reaction. Our results predict, however, that attachment of C^+ to the hydroxyl group of formic acid is only 0.6 kcal/mol less favorable than attachment to the carbonyl group, and that this attachment induces a direct dissociation of the system into HCO^+ and $COH^\bullet$. Therefore, we must conclude that the formation of $COH^\bullet$ as a product of the reaction cannot be discarded, although in both mechanisms (I and V) the cationic species formed (HCO^+) is the same. Also in agreement with the experimental evidence, no formation of COH^+ cation should be expected due to the large activation barrier associated with mechanism IV.

Unimolecular Reactivity of the Global Minimum. It can be observed that the energy profile described above does not include the global minimum of the $[H_2, C_2, O_2]^+$ PES, **1a**. In fact it is difficult to envisage a mechanism that would easily connect the adducts to the carbonyl or to the OH groups of formic acid with the insertion of the monocation into the C═O bond. Apparently, the most suitable mechanism would be one connecting the adducts to the carbonyl group (**8a**−**d**) with the complexes **4a,b**, through the cleavage of the C−OC bond and subsequent reorientation of the CO molecule. However, we were not able to locate the transition state for this process using the standard procedures. In view of these difficulties we studied the potential energy corresponding to this bond cleavage by fully optimizing the structure of the **8a** molecular ion for different C−OC distances. The results of this scan have been plotted in Figure 5. It can be seen that the curve presents a sharp maximum for a C−OC distance of 1.580 Å. However, the structure corresponding to this maximum is not a transition state but a saddle point of second order. One of its imaginary frequencies (886i cm^{-1}) corresponds indeed to the stretching of the C−OC bond, which is being dissociated, but there is another imaginary frequency (85i cm^{-1}) associated with the flipping of the $HCOH^+$ moiety. Actually, it can be observed that while in structure **8a** the HCOH and the CO subunits are coplanar, in species **4** the CO molecule is almost perpendicular to the HCOH plane. The conclusion is that the curve shown in Figure 5 corresponds to the superposition of two potential energy curves, which do not intersect because they lie on different potential energy surfaces. In other words, there are two different states for the same C−OC distance, one in which the CO fragment lies in the same plane of the HCOH moiety, and another in which it lies in a perpendicular plane. Hence, we must conclude that the C−OC distance is not the unique reaction coordinate connecting structures **8a** and **4a**.

In any case it is important to emphasize that this second-order saddle point lies about 18 kcal/mol above the adduct **8a**. This value is much higher than the energetic barriers associated with mechanisms I and V, and therefore the formation of the global minimum from the adducts of C^+ to formic acid cannot compete with the unimolecular dissociation of these adducts into $HCO^\bullet + HCO^+$. This is consistent with the fact that experimentally the $HCOH^+$ cation has not been detected as a product of the $C^+ + HCOOH$ reaction, although it should be the dominant product of the unimolecular decomposition of the global minimum **1a**. As shown in Figure 6, species **1a** may evolve through the **TS4a1a** transition state to yield structure **4a**, which would eventually dissociate into $CO + HCOH^+$ (mechanism A). A 1,2H shift connects also the global minimum with species **5c** (mechanism B) , which would dissociate into $HCO^\bullet + COH^+$. Alternatively, the isomerization **1a**−**1b**, implies

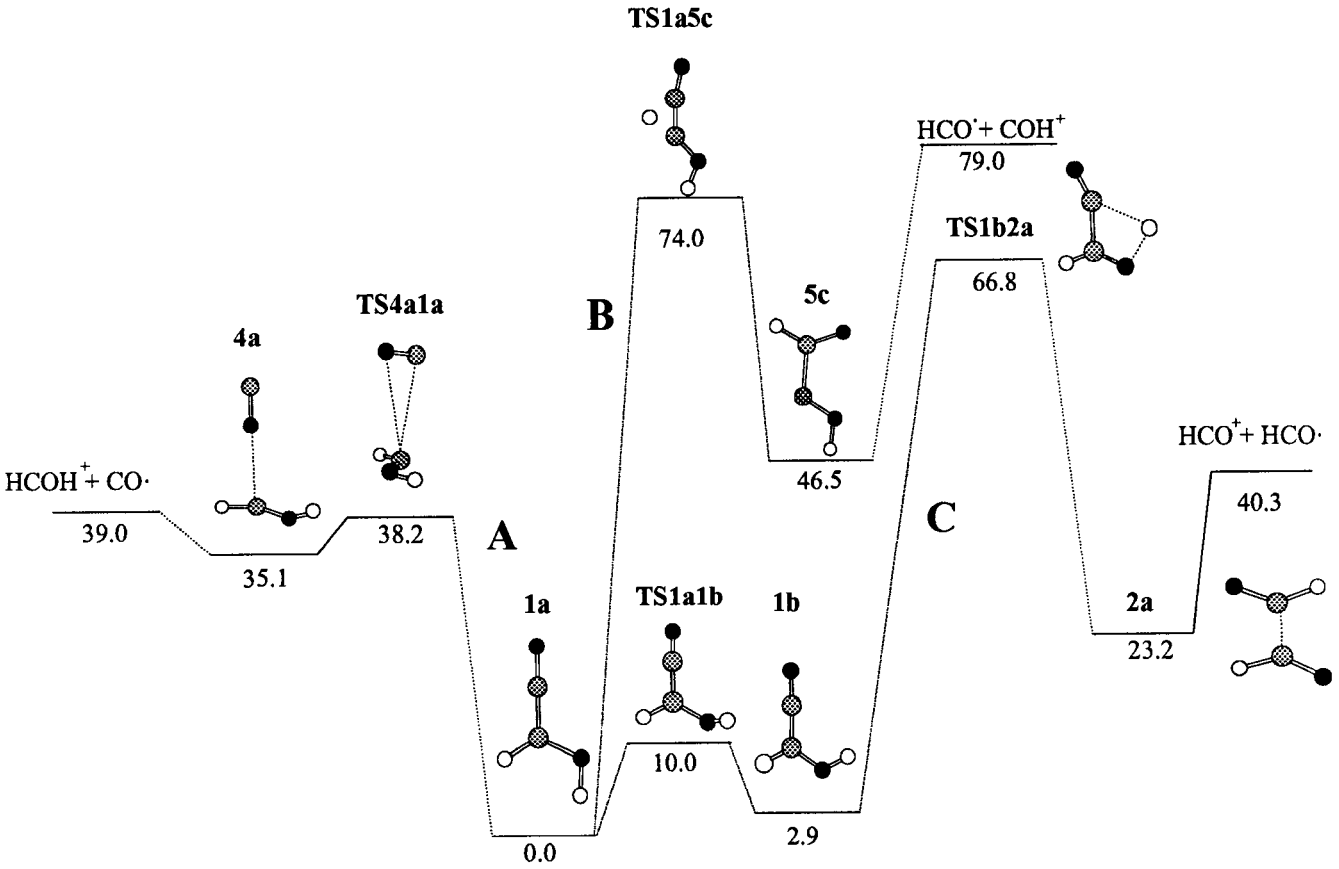

Figure 6. Energy profile corresponding to the unimolecular decomposition of the global minimum **1a** of the $[H_2, C_2, O_2]^+$ PES. Relative energies in kcal/mol.

a low-barrier OH internal rotation. Once the species **1b** is formed, a 1,3H shift, involving the **TS1b2a** transient species, would yield structure **2a**, which dissociates into $HCO^+ + HCO^\bullet$ (mechanism C). Since the barriers involved in mechanisms B and C are very high as compared with those involved in mechanism A, this must be the dominant process, leading to the loss of CO. The fact that no loss of CO has been experimentally observed ratifies that the formation of the global minimum **1a**, from species **8**, cannot compete with the reactive channel V leading to $HCO^\bullet + HCO^+$ as dominant products.

It is also worth noting from Figure 6 that the reaction $COH^+ + HCO^\bullet$ would yield $HCOH^+ + CO$, through the formation of species **5c** and **1a**. However, a similar process in which the COH^+ ion is replaced by HCO^+ would not occur in the gas phase because, as shown in the same figure, the **2a**−**1b** isomerization barrier lies higher in energy than the entrance channel.

Heats of Formation. From our G2 calculations good estimates of the heats of formation of the ionic products of $C^+ +$ formic acid reactions can be obtained. For this purpose we have considered the following processes:

$$C^+ + HCOOH \rightarrow HCO^+ + HCO^\bullet \qquad \Delta H^\circ_{298} = -130.6 \text{ kcal/mol} \quad (1)$$

$$C^+ + HCOOH \rightarrow COH^+ + HCO^\bullet \qquad \Delta H^\circ_{298} = -91.7 \text{ kcal/mol} \quad (2)$$

$$C^+ + HCOOH \rightarrow HCOH^+ + CO \qquad \Delta H^\circ_{298} = -132.4 \text{ kcal/mol} \quad (3)$$

The enthalpies of formation of species HCO^+, COH^+, and $HCOH^+$ can be deduced when the G2 enthalpies of reactions 1−3 are combined with the experimental enthalpies of formation of HCOOH, $HCO^\bullet$, CO, and C^+ taken from ref 13. The estimated heat of formation for HCO^+ is 199.2 kcal/mol, which is in good agreement with the experimental value (197.3 kcal/mol). For COH^+ our estimate (238.1 kcal/mol) is close to a reported value of 230 kcal/mol deduced from correlation with the oxygen 1s binding energy. The heat of formation predicted for $HCOH^+$ is 234.5 kcal/mol. For this system no values have been reported in the literature so far, but we are confident in the reliability of this value in view of the nice agreement found between our theoretical estimate and the experimental value for the particular case of HCO^+.

Conclusions

The most stable species of the $[H_2, C_2, O_2]^+$ PES is the structure **1a**, which can be viewed as the result of inserting the C^+ monocation into the C═O bond of formic acid. However, the products of the $C^+ +$ HCOOH reactions do not arise from the unimolecular decomposition of this species but from the structures that correspond to the attachment of C^+ either to the carbonyl oxygen atom or to the OH group of the neutral. Since both attachment processes are almost equally exothermic, the dominant products should be HCO^+, $HCO^\bullet$, and $COH^\bullet$. This is in agreement with the fact that HCO^+ is the sole product molecular ion detected in this reaction.

The unimolecular decomposition of the global minimum would yield, as the dominant product, $HCOH^+$ cation, which is not experimentally observed. This is consistent with our results, which show that the isomerization from the carbonyl oxygen adduct **8a** toward the global minimum **1a** cannot compete with the unimolecular decomposition of **8a** into $HCO^+ + HCO^\bullet$.

The two functional groups present in formic acid perturb each other to a significant extent, and the attachment of C^+ to both the carbonyl group or the hydroxyl group is less exothermic than the analogous processes in formaldehyde and methanol. A similar conclusion applies to the insertion mechanisms into the C═O or the C—OH bonds. The most important consequence of these changes is that while the insertion of C^+ into the C═O bond of formaldehyde is about 11 kcal/mol more exothermic than its insertion into the C—OH of methanol, in formic acid the gap between both process widens significantly (46.5 kcal/mol). On the other hand, while the attachment of C^+ to the OH group of methanol is 18 kcal/mol less exothermic than its addition to the C═O group of formaldehyde, in formic acid both processes are almost equally exothermic.

Significant differences are also observed with respect to Si^+ reactions. In formic acid + Si^+ reactions the insertion of the monocation into the C—OH linkage is the most favorable process, rather than the insertion into the C═O bond, which in turn is less favorable than the addition to the carbonyl oxygen atom.

This work has been partially supported by the DGES Project No. PB96-0067. A generous allocation of computing time at the Centro de Computación Científica de la Facultad de Ciencias (CCCFC) de la UAM is gratefully acknowledged. A.I.G. acknowledges a grant from the Ministerio de Educación y Cultura.

References and Notes

(1) (a) Amekraz, B.; Tortajada, J.; Morizur, J. P.; González, A. I.; Mó, O.; Yáñez, M. *J. Mol. Struct. (THEOCHEM)* **1996**, *371*, 313. (b) González, A. I.; Mó, O.; Yáñez, M. *Anal. Quim. Int. Ed.* **1997**, *93*, 310. (c) González, A. I.; Mó, O.; Yáñez, M. *Int. J. Mass Spectrom. Ion Processes* **1998**, *179*/*180*, 77. (d) Esseffar, M.; Luna, A.; Mó, O.; Yáñez, M. *J. Phys. Chem.* **1993**, *97*, 6607. (e) Esseffar, M.; Luna, A.; Mó, O.; Yáñez, M. *Chem. Phys. Lett.* **1993**, *209*, 557. (f) Esseffar, M.; Luna, A.; Mó, O.; Yáñez, M. *J. Phys. Chem.* **1994**, *98*, 8679. (g) Esseffar, M.; Luna, A.; Mó, O.; Yáñez, M. *Chem. Phys. Lett.* **1994**, *223*, 240. (h) Esseffar, M.; Luna, A.; Mó, O.; Yáñez, M. *Int. J. Quantum Chem.* **1996**, *57*, 559. (i) Luna, A.; Mó, O.; Yáñez, M. *Chem. Phys. Lett.* **1992**, *197*, 581. (j) Luna, A.; Mó, O.; Yáñez, M. *J. Mol. Struct. (THEOCHEM)* **1994**, *310*, 135. (k) Luna, A.; Yáñez, M. *J. Phys. Chem.* **1993**, *97*, 10659. (l) Gonzalez, A. I.; Yáñez, M. *Chem. Phys. Lett.* **1996**, *248*, 102.

(2) Mayer, P. M.; Parkinson, C. J.; Smith, D. M.; Radom, L. *J. Chem. Phys.* **1998**, *108*, 604.

(3) Turner, J. L.; Dalgarno, A. *Astrophys. J.* **1977**, *213*, 386.

(4) Leger, A.; Puget, J. L. *Astron. Astrophys.* **1984**, *137*, L5.

(5) Freeman, C. G.; Harland, P. W.; McEwan, M. J. *Aust. J. Chem.* **1978**, *31*, 2593.

(6) Raghavachari, K.; Trucks, G. W.; Pople, J. A. *J. Chem. Phys.* **1991**, *94*, 7221.

(7) Curtiss, L. A.; Raghavachari, K.; Redfern, P. C.; Pople, J. A. *J. Chem. Phys.* **1997**, *106*, 1063.

(8) Curtiss, L. A.; Raghavachari, K.; Redfern, P. C.; Pople, J. A. *Chem. Phys. Lett.* **1997**, *270*, 419.

(9) Frisch, M. J.; Trunks, G. W.; Schlegel, H. B.; Gill, P. M. W.; Johnson, B. G.; Robb, M. A.; Cheeseman, J. R.; Keith, T. A.; Peterson, G. A.; Montgomery, J. A.; Raghavachari K.; Al-Laham, M. A.; Zakrzewski V. G.; Ortiz, J. V.; Foresman, J. B.; Ciolowski, J.; Stefanow, B. B.; Nanayaklara, A.; Challacombe, M.; Peng, C. Y.; Ayala, P. Y.; Chen, W.; Wong, M. W.; Andres, J. L.; Replogle, E. S.; Gomperts, R.; Martin, R. L.; Fox, D. J.; Binkley, J. S.; Defrees, D. J.; Baker, J.; Stewart, J. P.; Head-Gordon, M.; González, C.; Pople, J. A. GAUSSIAN 94 (Rev. B. 1); Gaussian, Inc.: Pittsburgh, PA, 1995.

(10) Bader, R. F. W. *Atoms and Molecules. A Quantum Theory*; Clarendon Press: Oxford, U.K., 1990.

(11) The AIMPAC programs package has been provided by J. Cheeseman, and R. F. W. Bader.

(12) (a)Wiberg, K. B.; Hadad, C. M.; Rablen, P.; Cioslowski, J. *J. Am. Chem Soc.* **1992**, *114*, 8644. (b) Wiberg, K. B.; Nakaji D. *J. Am. Chem. Soc.* **1993**, *115*, 10658. (c) Wiberg, K. B.; Rablen, P. *J. Am. Chem. Soc.* **1995**, *117*, 2201.

(13) Lias, S. G.; Bartmess, J. E.; Liebman, L. F.; Holmes, J. L.; Levin R. D.; Mallard, W. G. *J. Phys. Chem. Ref Data* **1988**, *17*, 1.